Advanced Journal of Chemistry, Section A, 2026, 9(6), 997-1013

Advanced Journal of Chemistry, Section A

Journal homepage: www.ajchem-a.com

Original Research Article

β-Cyclodextrin-Based Metal–Organic Framework as a Novel Functional Bioactive Carrier: A Study for Quercetin Delivery

Muhammad Furqon Novryan Saputra[1], Aliyah Nabila[1], Madyawati Latief[1], Ayu Nadila Safitri[1], Indra Lasmana Tarigan[1,2] *

[1]*Department of Chemistry, Faculty of Science and Technology, Universitas Jambi, Jambi, 36361, Indonesia*

[2]*Natural Product and Bioactive Compound Laboratory, Faculty of Science and Technology, Universitas Jambi, Jambi, 36361, Indonesia*

ARTICLE INFO

Article history

Submitted: 2025-11-09
Revised: 2025-12-06
Accepted: 2025-12-31
ID: AJCA-2511-1966
DOI: **10.48309/AJCA.2026.558546.1966**

KEYWORDS

Quarcetin
β-Cyclodextrine-MOF
Drug delivery system
Novel functional

ABSTRACT

Quercetin is a natural flavonoid with strong antioxidant and therapeutic potential; yet, its practical use is hindered by poor aqueous solubility. To overcome this limitation, this study develops a functional carrier system based on a β-cyclodextrin metal–organic framework (β-CD-MOF) modified with cetyltrimethylammonium bromide (CTAB). In this design, CTAB acts as a surface-active modifier that improves the interaction between quercetin and the framework, while β-cyclodextrin provides hydrophobic cavities capable of accommodating bioactive molecules. Structural and morphological characterizations using FTIR, XRD, SEM, and PSA confirm the successful synthesis and modification of the material. *In vitro* release studies reveal a biphasic and controlled release profile, accompanied by a notable improvement in quercetin solubility compared to its free form. Overall, these findings demonstrate that CTAB-modified β-CD-MOF effectively encapsulates quercetin and enhances its dissolution behavior, highlighting its potential as a promising carrier system for hydrophobic compounds.

GRAPHICAL ABSTRACT

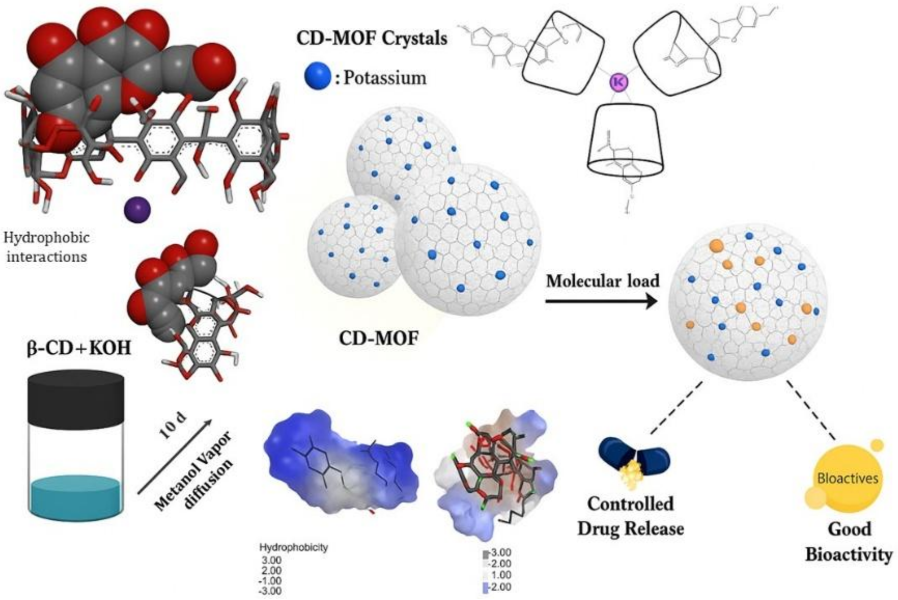

* Corresponding author: Indra Lasmana Tarigan
✉ E-mail: indratarigan@unja.ac.id

Introduction

Over the past few decades, metal–organic frameworks (MOFs) have emerged as a prominent class of porous crystalline materials owing to their modular architectures and exceptional physicochemical properties [1–3]. Constructed from the coordination of metal ions or clusters with organic linkers, MOFs offer high surface areas, tunable porosity, and structural versatility, enabling broad applications in gas storage, catalysis, separation, sensing, and drug delivery [2,4,5]. Recent developments in the biomedical field have focused on designing biocompatible MOFs using endogenous or pharmaceutically acceptable ligands—such as amino acids, carbohydrates, and oxalates—paired with biologically relevant metal ions including Na^+, K^+, and Cs^+. These strategies enhance safety profiles and expand the potential of MOFs for clinical translation [5,6].

Among the various biocompatible systems, β-cyclodextrin–based MOFs (β-CD-MOFs) have gained increasing interest due to their intrinsic biocompatibility, renewable origin, and unique host–guest inclusion capabilities. Incorporating β-cyclodextrin (β-CD) units into a crystalline framework not only preserves their molecular encapsulation ability, but also enhances stability, loading capacity, and controlled release performance. Several studies have demonstrated the versatility of β-CD-MOFs as drug carriers. For instance, CTAB-modified β-CD-MOFs synthesized via vapor diffusion have been used for emodin delivery [7,8], while more recent work has shown significant improvements in curcumin delivery and targeted anticancer activity using β-CD-MOF systems. These findings highlight the potential of β-CD-MOFs as effective platforms for delivering hydrophobic therapeutics [8,9].

Quercetin, a naturally occurring dietary flavonoid abundant in fruits and vegetables such as apples, onions, and tea, exhibits a wide spectrum of pharmacological activities, including antioxidant, anti-inflammatory, cardioprotective, neuroprotective, and anticancer effects [10,11]. However, despite its therapeutic potential, the clinical use of quercetin is severely limited by its extremely low oral bioavailability (<2%). This limitation arises from poor aqueous solubility, limited intestinal permeability, rapid metabolism, and extensive first-pass biotransformation into less active conjugates [12]. Although various delivery strategies—such as nanoparticles, lipid-based carriers, and cyclodextrin complexes—have been investigated to improve its solubility and absorption, challenges remain in achieving high loading efficiency, structural stability, and controlled release.

Given the hydrophobic nature of quercetin and the structural characteristics of β-CD-MOFs, these materials present a promising approach for enhancing quercetin delivery. However, studies investigating the molecular interactions, loading behavior, and physicochemical performance of quercetin-loaded β-CD-MOF systems remain limited. In particular, the effects of structural modification on the encapsulation efficiency and release dynamics of quercetin have not been comprehensively explored.

Therefore, this study focuses on the synthesis and characterization of a β-CD-MOF carrier system for quercetin delivery. its structural and physicochemical properties, loading capacity, and release behavior were evaluated to provide new insights into the feasibility of β-CD-MOF as a biocompatible platform for improving the solubility, stability, and bioavailability of hydrophobic bioactive compounds.

Experimental

Materials and instrumentation

The materials utilized in this study include β-cyclodextrin (Sigma-Aldrich), potassium hydroxide (KOH) (Sigma-Aldrich), methanol (ProAnalytic), ethanol (ProAnalytic), isopropyl alcohol (ProAnalytic), distilled water, quercetin

(Sigma Aldrich), 2,2-diphenyl-1-picrylhydrazyl (DPPH) (Sigma-Aldrich), and phosphate-buffered saline (PBS, pH 7.4) (Sigma-Aldrich). All chemicals were of analytical grade and used without further purification unless otherwise stated. Distilled water was used throughout the experimental procedures.

The instrumentation employed in this research consists of standard laboratory glassware and various analytical and processing equipment, including an orbital shaker (BalMed), a hot plate (Thermo Fisher Scientific), an oven (Thermo Fisher Scientific), syringe filters, and a centrifuge (Thermo Fisher Scientific). Characterization of the samples was performed using Fourier transform infrared spectroscopy (FTIR) (Thermo Fisher Scientific), Particle size analyzer (PSA) (Beckman Coulter), Scanning Electron Microscopy equipped with Energy-Dispersive X-ray Spectroscopy (SEM-EDX) (Thermo Fisher Scientific), X-ray Diffraction (XRD) (Thermo Fisher Scientific), and Ultraviolet–Visible (UV–Vis) spectrophotometry (Thermo Fisher Scientific). All instruments were calibrated prior to use to ensure accuracy and reproducibility of the measurements.

Method

Synthesis of β-CD-MOF

β-CD-MOF was synthesized using a vapor-diffusion crystallization method (Figure 1). First, 141.875 mg of β-cyclodextrin (0.125 mmol) was dissolved in 5.0 mL of KOH solution (200 mmol/L) under continuous stirring at 500 rpm for 30 min to ensure complete dissolution and formation of β-CD–K^+ complexes. The resulting solution was then filtered through a 0.45 µm syringe filter to remove any undissolved particulates, after which 0.5 mL of methanol was added to initiate the pre-nucleation process. The filtrate was placed in a sealed vessel and exposed to methanol vapor by positioning the vessel inside a beaker containing 45 mL of methanol. This setup was oven-heated at 50 °C for 6 h , yielding a clear β-CD–KOH precursor solution [13].

Subsequently, 7 mL of the β-CD–KOH solution was transferred into a clean container, and 5 mL of CTAB solution (8 mg/mL) was rapidly added to promote framework assembly and crystal growth. The mixture was incubated at room temperature overnight to allow the formation of β-CD-MOF crystals. After the appearance of white crystalline material, the solid was collected and washed three times with isopropanol and methanol (2 × 30 mL) to remove residual CTAB and unreacted components. Finally, the product was dried under vacuum at 40 °C overnight to obtain purified β-CD-MOF.

Preparation of quercetin-loaded β-CD-MOF

The incorporation of quercetin into β-cyclodextrin metal–organic framework (β-CD-MOF) was achieved using the impregnation method. In a typical procedure, 30 mg of β-CD-MOF was dispersed in 10 mL of an ethanolic solution of quercetin (2 mg/mL), corresponding to a quercetin-to-β-CD-MOF weight ratio 2:3 [8]. The resulting suspension was agitated using an orbital shaker at a speed of 150 rpm for 48 h to facilitate the adsorption process. After the incubation period, the obtained inclusion complex was separated by centrifugation and washed several times with ethanol to remove any unbound quercetin. The purified quercetin-loaded β-CD-MOF was then dried in an oven at 40 °C overnight to ensure complete solvent evaporation. The dried sample was subsequently stored in a desiccator until further characterization [13].

Characterization

The synthesized β-cyclodextrin metal–organic framework (β-CD-MOF) and the quercetin-loaded β-CD-MOF were characterized using several analytical techniques to confirm their structures.

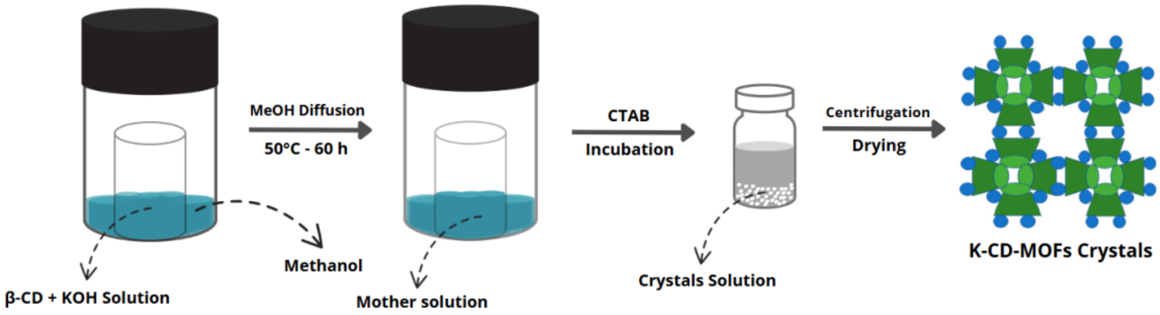

Figure 1. Schematic diagram of Synthesis of β-CD-MOF

Characterization

The synthesized β-cyclodextrin metal–organic framework (β-CD-MOF) and the quercetin-loaded β-CD-MOF were characterized using several analytical techniques to confirm their structural, morphological, and physicochemical properties. The crystalline structure of the materials was analyzed using XRD to identify the characteristic diffraction peaks and to verify the successful formation of the β-CD-MOF framework. The surface morphology and elemental composition were examined using Scanning Electron Microscopy coupled with Energy-Dispersive X-ray Spectroscopy (SEM-EDX), providing insights into particle shape, surface texture, and elemental distribution. In addition, the particle size distribution and average particle diameter were determined using a PSA to assess the homogeneity and dispersion of the synthesized materials. The FTIR analysis was performed to identify the functional groups present and to confirm the successful coordination between β-cyclodextrin and the metal ions. Finally, Ultraviolet–Visible (UV–Vis) spectrophotometry was employed to evaluate the encapsulation efficiency and release behavior of quercetin within the β-CD-MOF matrix.

In silico analysis of Q-CD-MOF interactions with the 1HD2 receptor

An *in silico* study was conducted to evaluate the molecular interactions of quercetin and β-cyclodextrin–K-MOF with the selected immune-related receptor CBTau-28.1 (PDB ID: 5ZV3). Network pharmacology screening using SwissTargetPrediction, GeneCards, STRING, PubChem, and Venny was performed to identify relevant biological targets prior to receptor selection. Receptor preparation was carried out in BIOVIA Discovery Studio by removing crystallographic water molecules and native ligands, followed by structural optimization. Ligand structures were built and energy-minimized using Chem3D before being converted into docking-compatible formats. Molecular docking simulations were then performed using BIOVIA Discovery Studio and PyRx, with the optimal ligand pose determined based on the lowest predicted binding energy. The best docking conformation was further analyzed to characterize interacting amino acid residues, hydrogen bond interactions, predicted inhibition constants, and binding free energies [14].

Drug release the mimic bodys, pH

The *in vitro* drug release of quercetin was studied in neutral (pH 7.4, blood) and acidic (pH 1.2, stomach) media. A total of 5.5 mg of Qr-β-CD-

MOF was added to 3 ml of PBS buffer for 5 min. Aliquots (2 ml) were withdrawn at different time intervals (5, 15, 30, 60, 90, and 120 min) and replaced with fresh buffer. After subsequent dilution, the samples were analyzed using a UV-Visible spectrophotometer at 374 nm [8]. The drug release was calculated using Equation (1).

$$\text{Drug release \%} = \frac{C_f - C_0}{C_i} \qquad (1)$$

DPPH Radical scavenging assay

The antioxidant activity of the samples was evaluated using the 2,2-diphenyl-1-picrylhydrazyl (DPPH) free radical scavenging assay, following the procedure described by [17] with slight modifications. A DPPH solution was prepared at a concentration of 40 ppm in methanol. The test samples, consisting of pure quercetin, β-CD-MOF, and quercetin-loaded β-CD-MOF (Qr-β-CD-MOF), were prepared at concentrations of 10, 8, 6, 4, and 2 µg/mL. An aliquot of 3 mL of DPPH solution was mixed with each sample solution. The mixtures were then homogenized and incubated in the dark at 37 °C for 25 min to allow the reaction between DPPH radicals and the antioxidant compounds. After incubation, the absorbance of each mixture was measured at 517 nm using a UV–Vis spectrophotometer [15]. The DPPH radical scavenging activity (%) was calculated using Equation (2):

$$\text{DPPH radical scavenging activity (\%)} = \{1-(A-Ao)/A1\} \times 100 \qquad (2)$$

Histopatology analysis

The *in vivo* study was conducted using male white Wistar mice. A total of three mice were acclimatized for seven days prior to experimentation. The animals were then divided into three groups: the negative control group [K(–)], which received no treatment; the positive control group [K(+)], which was administered quercetin alone; and the treatment group [P1], which was administered quercetin-CD-MOF. On day 8, all mice in the treatment protocol received quercetin-CD-MOF at a dose of 10 mg/kg body weight. The administration was performed seven times using the oral gavage method. Following treatment, histopathological examination was carried out on the liver tissue of the mice [16].

Result and Discussion

3D visualization and structural analysis of quercetin-loaded CD-MOF

To comprehensively understand the structural behavior of quercetin encapsulated in CD-MOF, both experimental characterization and computational modeling were utilized. β-Cyclodextrin-based metal–organic frameworks (β-CD-MOF) represent an innovative subclass of hybrid porous materials that combine the host–guest selectivity of β-cyclodextrin (β-CD) with the rigidity and high porosity of metal–organic frameworks (MOF) β-Cyclodextrin is a cyclic oligosaccharide composed of seven α-1,4-linked D-glucopyranose units, forming a toroidal structure with hydrophobic cavity interior that favors the inclusion of hydrophobic guests and hydrophilic exterior due to primary (C6–OH) and secondary (C2, C3–OH) hydroxyl groups [16]. These hydroxyl groups can participate in coordination with metal cations, enabling the β-CD to act as a multidentate organic ligand in framework formation.

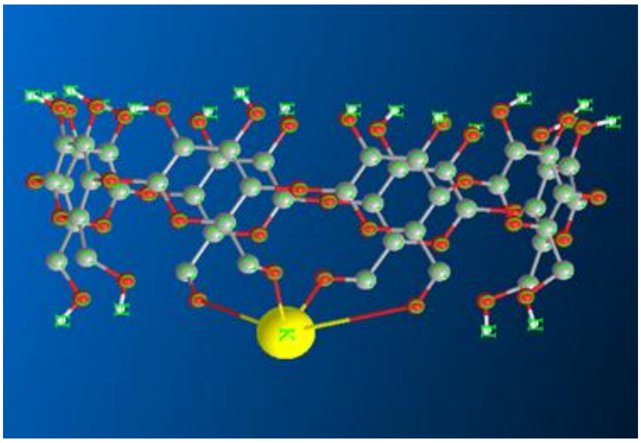

Figure 2. Schematic representation of the formation mechanism of β-cyclodextrin metal–organic framework (β-CD-MOF)

In the formation of β-CD-MOF, metal ions such as K^+ interact with the secondary hydroxyl groups of β-CD through coordination bonds (Figure 2) [13]. The resulting crystalline framework often adopts a cubic structure, with β-CD molecules serving as linkers arranged in three-dimensional porous networks [17]. Further studies have performed by Guo *et al.* [18]; this framework can possess surface area up to 680 m^2/g, pore volume of 0.40-0.50 cm^3/g and pore size centered around 1.2-1.5 nm.

Quercetin, a naturally occurring flavonoid found in various fruits and vegetables, has attracted substantial scientific interest due to its potent antioxidant, anti-inflammatory, and anticancer properties. However, its clinical translation remains limited by poor aqueous solubility, low bioavailability, and rapid metabolic degradation [19]. Herein the CD-MOF provides a good solution for enhancing its delivery.

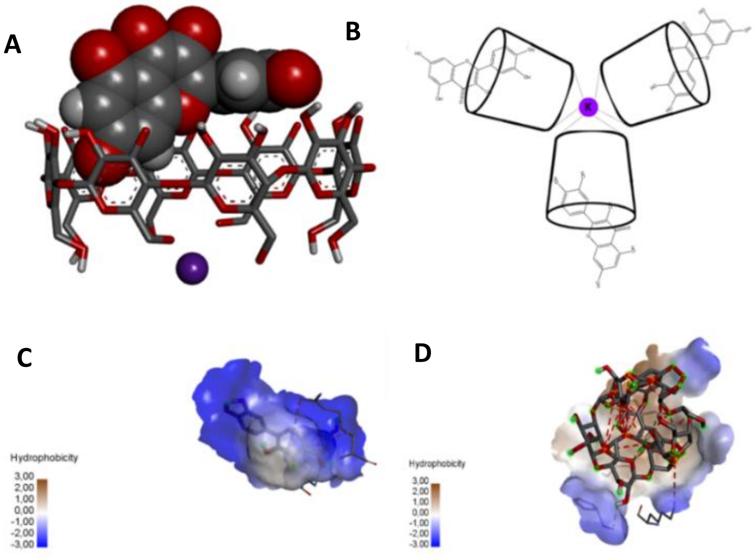

Figure 3. Structural representation of the hydrophobic interactions in β-CD-MOF capsules: (A–B) molecular configuration and assembly of β-cyclodextrin units; (C–D) hydrophobic surface analysis indicating the interaction regions between quercetin and β-CD-MOF

Table 1. Binding affinity and hydrogen bonding

Type	Binding affinity	Total hydrogen-bond	Binding residue
Q-CD-MOF	-8.6	6	Leusin (LSN) Prolin (PRO) Valin (VAL)
Quercetin	-7.1	4	Asparagin (ASN) Glutamin (GLU)

The modeling results show that the Q-CD-MOF complex has a higher binding affinity than free quercetin, at −8.6 kcal/mol and −7.1 kcal/mol, respectively (Table 1). This increase in affinity is supported by the number of hydrogen bonds formed, with Q-CD-MOF producing six hydrogen bonds, compared to free quercetin, which forms only four bonds. In addition, Q-CD-MOF interacts with non-polar Leucine (LSN), Proline (PRO), and Valine (VAL) residues, contributing to more stable hydrophobic interactions. Meanwhile, free quercetin only interacts with the polar residues Asparagine (ASN) and Glutamine (GLU), which are relatively weaker in terms of interaction stability. Overall, these findings indicate that the encapsulation of quercetin in CD-MOF can increase the strength and stability of interactions with targets, thereby supporting the potential of Q-CD-MOF as a more effective delivery system (Figure 4).

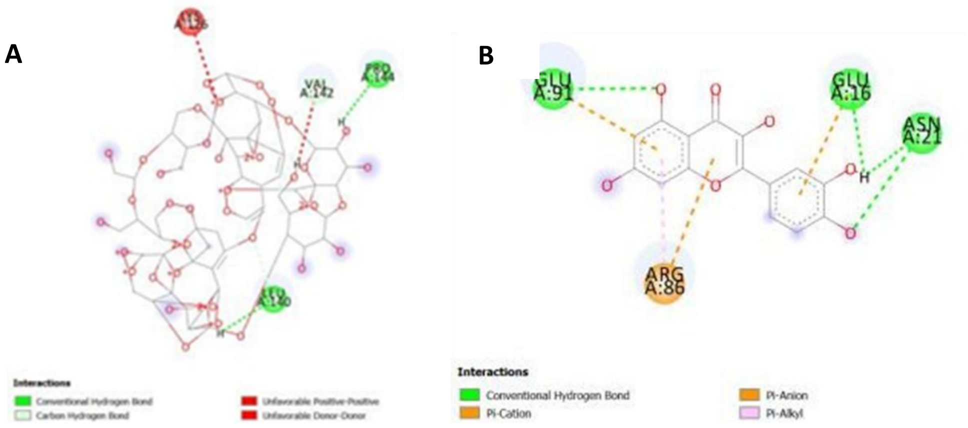

Figure 4. Ligand interaction with protein target (A) Q-CD-MOF and (B) quarcetin

Quercetin is embedded within the cavity of CD-MOF. The encapsulated quercetin molecule, shown in a space-filling representation (Figure 3A), displays its planar polyphenolic core and hydroxyl substituents, suggesting multiple potential interaction points, including hydrogen bonding and π-π stacking. The CD-MOF reveals its porous, channel-like structure with hydrophobic cavities and hydrophilic portals formed by hydroxylated rims of the cyclodextrin units. A potassium ion can be seen stabilizing the framework, indicating the role of metal coordination in maintaining the supramolecular integrity (Figure 3B). Each cyclodextrin unit, composed of a cyclic oligosaccharide with a hydrophilic exterior, features multiple primary and secondary hydroxyl groups that can interact electrostatically with the K^+ ion. These hydroxyl groups serve as electron donors, forming coordinate bonds with the positively charged K^+ ion [8]. The flexible geometry and moderate charge density of potassium allow it to simultaneously coordinate with multiple oxygen atoms from different CD units, facilitating the assembly of a robust 3D framework. Moreover, the inclusion of K^+ ions enhances the structural integrity and porosity of the framework by promoting intermolecular hydrogen bonding and stabilizing the spatial orientation of the CD [17]. Figure 3C shows the hydrophilicity-dominated surface of free quercetin, mainly due to the hydroxyl groups. However, despite these polar functionalities, quercetin remains poorly soluble in water and exhibits limited oral bioavailability due to its planar aromatic structure and tendency to aggregate in aqueous environments [18]. In contrast, Figure 3D illustrates a more hydrophobic and neutral surface after encapsulation within CD-MOF, as many polar groups become buried or involved in internal interactions. This shift in surface polarity supports enhanced membrane permeability and improved bioavailability.

IR fingerprint interaction

To investigate the structural characteristics and verify the successful encapsulation of quercetin within the CD-MOF matrix, FTIR spectroscopy was performed on pure quercetin, quercetin-loaded CTAB-CD-MOF, functionalized CTAB-CD-MOF and CD-MOF (Figure 5, Table 2).

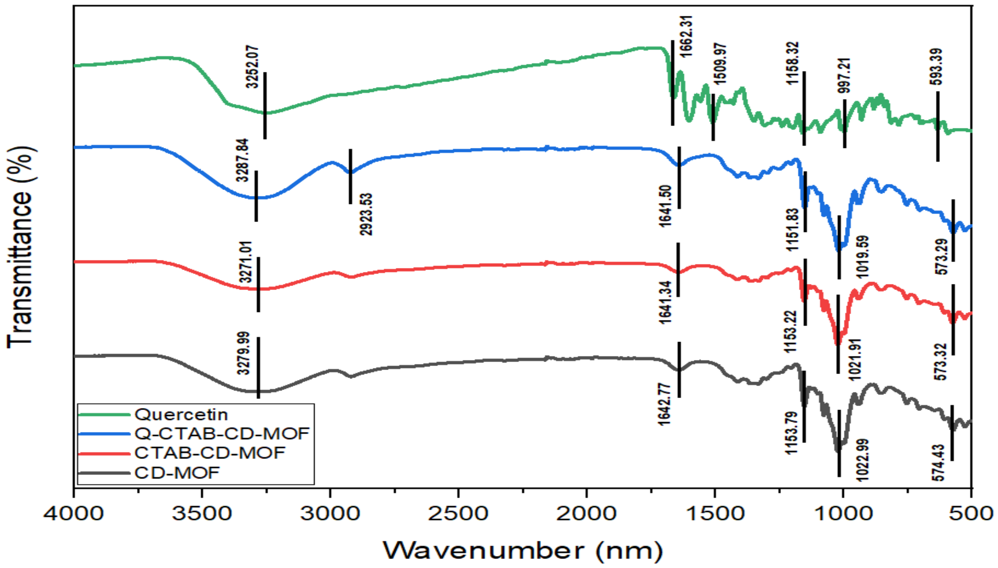

Figure 5. IR-spectra of β-CD-MOF, CTAB–CD-MOF, Q–CTAB–CD-MOF, and pure quercetin. The characteristic absorption bands indicate the functional groups associated with β-cyclodextrin and the successful incorporation of quercetin into the CD-MOF framework. Shifts in the O–H stretching and C=O vibration regions confirm the interaction between quercetin and the β-CD-MOF matrix

Table 2. Characteristic peak

Vibration	Quercetin	Q-CTAB-CD-MOF	CTAB-CD-MOF	CD-MOF
O-H	3252.07	3287.84	3271.01	3279.99
C-H stretching	-	3923.53	-	-
C=O	1662.31	1641.50	1641.34	1642.27
C=C stretching	1509.97	-	-	-
-O-C	1158.32	1151.81	1153.22	1153.79
C-O-C	997.21	1019.59	1021.91	1022.99
Fingerprint	593.39	573.29	573.32	574.43

The FTIR spectrum of pure quercetin exhibits characteristic vibrational bands at 3,262.07 cm^{-1} (phenolic O-H stretching), 1,662.31 cm^{-1} (C=O stretching of the flavonol carbonyl group), and 1,508.97 cm^{-1} and 1,165.83 cm^{-1} corresponding to aromatic C=C stretching and C-O-C bending, respectively [17]. These peaks reflect the functional groups responsible for quercetin's hydrogen bonding ability and its electron rich aromatic system. The CD-MOF spectrum shows a broad O-H stretching band at 3,279.99 cm^{-1}, consistent with the abundant hydroxyl groups of β-cyclodextrin and water molecules coordinated within the framework. Bands at 1,642.77 cm^{-1} and 1,022.39 cm^{-1} correspond to bending vibrations of confined water and the glycosidic C-O-C linkages of the cyclodextrin matrix, confirming the preservation of the CD ring structure within the MOF network [18]. These peaks define the baseline structure to which subsequent modifications must be compared.

Following CTAB functionalization, the CTAB-CD-MOF spectrum displays distinct C-H stretching bands at 2,923.53 cm^{-1} and 2,854 cm^{-1}, characteristic of the long alkyl chain of CTAB. A slight shift in the O-H stretching band (3,271.01 cm^{-1}) further indicates modification of the hydrogen bonding environment. Mechanistically, CTAB acts as a structure directing and surface capping agent. The cationic head group interacts with the negatively polarized surface of the CD-MOF, while the hydrophobic tail introduces an apolar microenvironment. This amphiphilic arrangement not only modulates crystal surface energy, but also facilitates subsequent host-guest interactions with hydrophobic molecules such as quercetin [14,19]. In the quercetin-loaded CTAB-CD-MOF composite, spectral changes provide strong evidence of encapsulation. Key quercetin bands including the O-H stretching and C=O stretching shift to 3,287.84 cm^{-1} and 1,644.50 cm^{-1}, accompanied by noticeable broadening. These modifications indicate the formation of hydrogen bonds and supramolecular interactions between quercetin and the hydroxyl CD cavities. Importantly, attenuation or partial disappearance of quercetin specific peaks at 1,508.97 cm^{-1} (C=C aromatic) suggests restricted vibrational freedom due to confinement within the host matrix [19].

Crystal analysis

The structural and morphological of crystals differences between CD-MOF and quercetin-loaded CD-MOF were further investigated using XRD and optical microscopy, as illustrated in Figure 6. Figure 6A shows the XRD patterns of pristine CD-MOF and quercetin-loaded CD-MOF (Q-CD-MOF). The characteristic sharp and intense peaks of CD-MOF in the 2θ range of 5°–35° confirm its high crystallinity and ordered porous structure. In contrast, Q-CD-MOF exhibits a noticeable decrease in peak intensity and slight broadening within the 18°–30° region, indicating a partial loss of crystallinity after quercetin encapsulation. This reduction is commonly observed in flexible MOF systems and can arise from guest incorporation, where quercetin molecules occupy the internal cavities and disrupt the regular packing of the β-CD framework, leading to the formation of localized amorphous domains caused by restricted molecular mobility within the pores [20,21]. Despite these changes, peak area integration shows that CD-MOF retains 99% crystallinity, while Q-CD-MOF maintains 95%, indicating that the material largely preserves its ordered structure and remains predominantly crystalline even after guest loading.

Figure 6B presents the optical microscopy image of the as-synthesized CD-MOF crystals, which exhibit transparent, well-defined rectangular prismatic shapes characteristic of a highly ordered framework. Following drug loading (Figure 6C), the crystals display a markedly different appearance, becoming more irregular, opaque, and showing a distinct yellow coloration attributable to quercetin incorporation. These

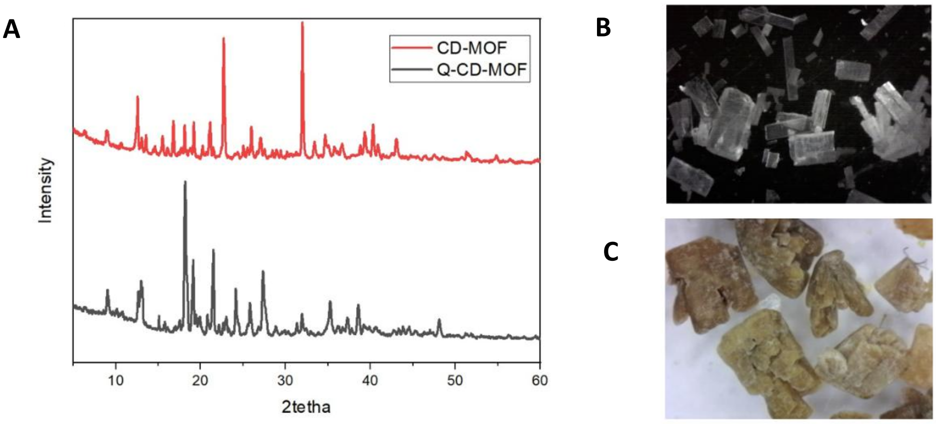

Figure 6. XRD patterns and morphological appearance of β-CD-MOF and quercetin-loaded β-CD-MOF (Q–CD-MOF). (A) XRD patterns of β-CD-MOF and Q–CD-MOF showing the characteristic diffraction peaks, confirming that the crystalline framework of β-CD-MOF was retained after quercetin incorporation. (B) and (C) represent the macroscopic morphology of β-CD-MOF and Q–CD-MOF, respectively, indicating the change in color and texture after quercetin loading

visual modifications indicate perturbations to both the external morphology and internal cavity environment of the CD-MOF, consistent with host–guest interactions that disrupt the original crystal packing. The observed changes are further corroborated by the IR analysis, which confirms the presence of quercetin-specific functional groups within the framework, supporting the conclusion that successful encapsulation has occurred.

SEM-EDS Analysis

The observed reduction in potassium signal, together with the altered morphology of Q-CD-MOF, indicates that quercetin loading not only introduces guest molecules into the cyclodextrin framework, but also induces subtle yet meaningful structural transitions. These transitions may arise from competitive coordination or surface adsorption processes, in which quercetin interacts with the cyclodextrin cavity through hydrogen bonding and hydrophobic interactions while simultaneously engaging with residual potassium ions within the MOF lattice [20]. Previous studies on cyclodextrin MOFs have demonstrated that guest molecules with high polarity and multiple hydroxyl groups—such as polyphenolic compounds—can perturb the primary coordination sphere and modify electron density distribution around metal centers, leading to measurable changes in elemental composition and crystal growth behavior [21,22].

In addition to structural changes, the incorporation of quercetin is expected to influence the physicochemical properties of CD-MOF. The irregular crystal morphology observed in Q-CD-MOF typically correlates with increased surface roughness and the presence of defect sites, which may enhance guest loading efficiency or modulate release kinetics (Figure 7) [23]. Such defects create additional microenvironments for molecular interaction, potentially improving the dispersion of quercetin within the framework. From a functional standpoint, these modifications could enhance the material's ability to protect quercetin from degradation and improve its bioavailability by enabling more controlled and sustained release. This is particularly important because quercetin is known to exhibit poor water solubility and limited stability under physiological conditions.

Moreover, the decrease in potassium concentration in Q-CD-MOF suggests that the material undergoes partial rearrangement of its coordination network to accommodate quercetin. This adaptability reflects the dynamic nature of cyclodextrin-based MOFs, which are recognized for their structural flexibility compared to traditional rigid MOFs. Such flexibility can be advantageous for drug delivery applications, as it allows the framework to adjust its pore environment to maximize host–guest compatibility without compromising structural integrity [5,24]. These findings imply that Q-CD-MOF may achieve an optimal balance between mechanical stability and molecular accessibility, enabling effective encapsulation while maintaining the ability to release quercetin in response to environmental stimuli [25,26].

Overall, the combined SEM and EDS results provide a comprehensive understanding of how quercetin influences both the composition and microstructure of CD-MOF. The successful formation of Q-CD-MOF is evidenced not only by changes in elemental distribution, but also by the morphological transitions that accompany guest incorporation. These insights collectively highlight the potential of Q-CD-MOF as a versatile nanocarrier system, capable of enhancing the physicochemical properties and therapeutic performance of quercetin.

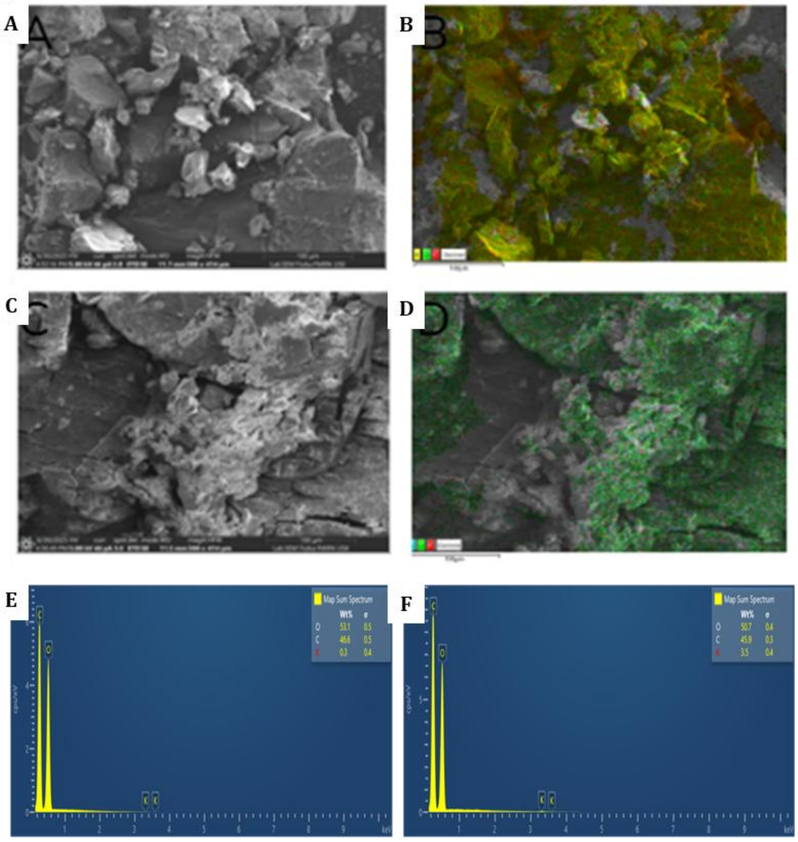

Figure 7. Scanning Electron Microscopy (SEM) and Energy-Dispersive X-ray (EDX) analyses of CD-MOF and Q-CD-MOF. Panels (A) and (B) show the SEM morphology and EDX elemental mapping of CD-MOF, respectively, illustrating aggregated crystalline particles and the distribution of constituent elements in the unloaded framework. Panels (C) and (D) present the SEM morphology and corresponding EDX elemental mapping of Q-CD-MOF, showing surface texture changes and confirming elemental dispersion after quercetin loading. Panel (E) displays the EDX weight percentage (wt%) profile of Q-CD-MOF, while Panel (F) presents the wt% profile of CD-MOF, serving as the compositional baseline prior to quercetin incorporation

Particle size of CD-MOF loaded Quarcetin

Particle Size Analysis (PSA) was performed to determine the mean size, size distribution, and uniformity of CD-MOF particles. The results indicated that CD-MOF exhibited a narrow and unimodal particle size distribution, with a mean particle diameter (D_{50}) of approximately 144.18 µm. This confirms that the material is within the microscale range, consistent with previous findings reported by a previous study observed CD-MOF crystals in the micrometer domain [27].

The relatively large crystal size can be attributed to the synthesis method employed. The vapor diffusion approach facilitates controlled crystal growth and promotes the formation of well-ordered, larger crystals. Furthermore, the inherently large molecular size of cyclodextrin (CD) and its coordination with potassium ions likely favor the formation of stable, extended frameworks, thereby reducing the likelihood of nanoparticle formation in the absence of additional modifications. Such uniform particle size distribution and microscale dimensions are advantageous for reproducible performance in subsequent applications, such as drug loading and release, as they ensure consistent diffusion and interaction profiles.

% Inhibition of DPPH radicals

The inhibitory performance of Q-CD-MOF was critically evaluated using DPPH assay to determine antioxidant activity comparison with free quercetin, CD-MOF, and the control sample, as illustrated in Figure 8.

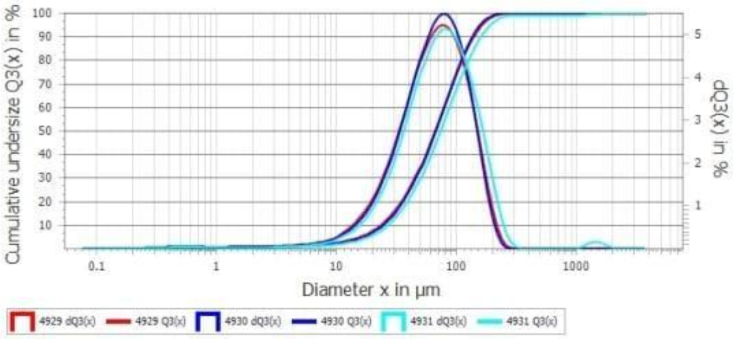

Figure 8. Particle size of CD-MOF

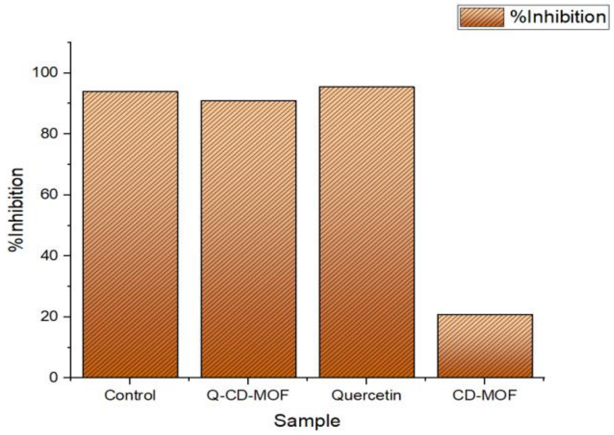

Figure 9. DPPH radical scavenging activity of β-CD-MOF, quercetin, and quercetin-loaded β-CD-MOF (Q–CD-MOF). The Q-CD-MOF exhibited high antioxidant activity comparable to pure quercetin, indicating the effective incorporation of quercetin within the β-CD-MOF framework, while the unloaded β-CD-MOF showed minimal inhibition

Free quercetin exhibited the highest inhibition percentage 95.40%, consistent with its potent antioxidative profile. Q-CD-MOF, which incorporates quercetin into CD-MOF, retained a comparably high inhibitory activity 90.92%, indicating that the biofunctionality of quercetin was largely preserved upon encapsulation. This finding strongly suggests that the structural integration of quercetin into the CD-MOF did not significantly compromise its bioactivity [4]. Instead, the encapsulation may offer additional advantages, such as enhanced stability, sustained release, and improved dispersibility of the active compound under physiological or environmental conditions [28]. A similar pattern was demonstrated by Sadeh *et al.* [9], who reported that *β*-CD-MOF loaded with curcumin showed antioxidant activity nearly equivalent to free curcumin, despite the compound being encapsulated within the cyclodextrin cavities. The findings emphasized that the host-guest interaction within *β*-CD-MOF does not diminish the intrinsic radical-scavenging capacity of the encapsulated polyphenol, but instead, helps stabilize the active compound against degradation.

Drug release behavior and LC%

Sustained-release behavior of Q-CD-MOF and its loading capacity percentage were calculated through *in vitro* experimental assays in two different simulated physiological environments and methanol.

As illustrated in Figure 9, both release profiles displayed a distinct biphasic pattern characterized by an initial burst release during the first 15–20 min, followed by a sustained slow-release phase extending up to 120 min. This release behavior correlates strongly with the mechanistic stages described in the Q-CD-MOF interaction pathway (Figure 10). The initial rapid release phase corresponds to the *host–guest recognition* and *surface-level interactions* shown in the mechanism figure (Figure 11). In this stage, quercetin molecules that are weakly associated with the MOF exterior—either through shallow insertion into the cyclodextrin torus or through weak surface adsorption—are released quickly due to minimal steric hindrance. These loosely bound molecules reside outside the deeply embedded sites represented in the *stabilization and encapsulation* phase of the mechanism. Similar early burst phenomena have been reported in MOF- and cyclodextrin-based carriers, where incomplete host–guest complexation or surface-localized drug fractions lead to rapid initial dissolution [2].

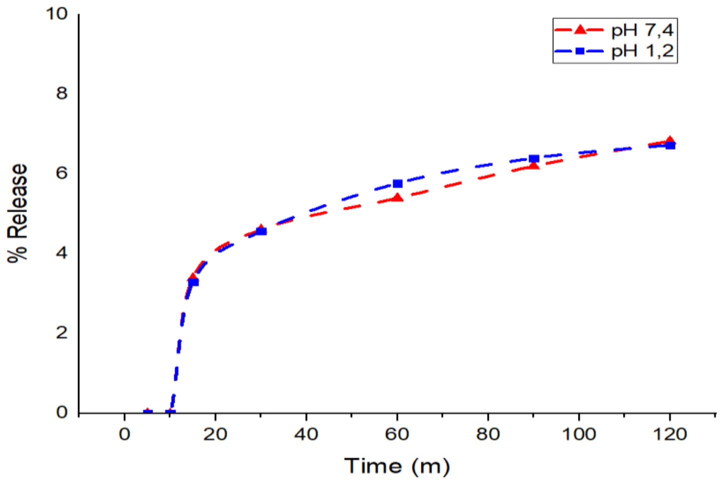

Figure 10. *In vitro* release profiles of quercetin from *β*-CD-MOF at pH 7.4 and pH 1.2, showing a burst release followed by a sustained release phase, with faster release observed under acidic conditions

Furthermore, the involvement of CTAB on the CD-MOF surface likely modulates the microenvironment by introducing a partially hydrophobic barrier around the framework, as suggested by the *framework adaptation* stage in Figure 11 mechanism. This barrier may restrict the immediate ingress of aqueous media into the deeper cavities of the material, thereby enhancing the contrast between fast-releasing surface-bound quercetin and the more strongly trapped molecules within the framework interior.

The second, slower release phase aligns with the encapsulation and stabilization stage illustrated in the mechanism schematic. Once the surface-associated quercetin has been depleted, the release becomes governed by diffusion from the internal cavities of the Q-CD-MOF, where quercetin is stabilized via hydrogen bonding, hydrophobic interactions, and partial disruption of K^+ coordination. These interactions, also depicted in the mechanistic diagram, contribute to stronger host–guest binding and require longer time for desorption or diffusion out of the framework. The sustained-release behavior observed up to 120 min, therefore, confirms the successful integration of quercetin into the CD-MOF matrix and validates the structural adaptation highlighted in the mechanism Figure 11.

Overall, the biphasic release profile not only demonstrates effective quercetin encapsulation, but also provides functional evidence supporting the molecular interactions proposed in the mechanistic model. The close correspondence between experimental release data and the predicted behavior from Figure 11 mechanism reinforces the conclusion that the Q-CD-MOF system operates through a combination of surface desorption and diffusion-mediated release from stabilized host–guest complexes.

Cytotoxicity assay

In this experimental study, the test animals were administered the treatment seven times at a dosage of 10 mg/kg body weight. Two days following the final administration, the mice were euthanized, and their hepatic tissues were excised for histopathological evaluation. The subsequent histological observations are presented in Figure 12. The liver plays a central role in numerous physiological processes, including glycogen storage, fat-soluble vitamin storage, fatty acid metabolism, synthesis of functional proteins (such as enzymes and plasma proteins), and the production of enzymes involved in xenobiotic metabolism [29]. Due to its unique structure and critical physiological functions, the liver is highly susceptible to chemical-induced toxicity. Most xenobiotics enter the body through the gastrointestinal tract, and following intestinal absorption, they are transported via the hepatic portal vein directly to the liver. Consequently, the liver is the first organ to be exposed to the highest concentrations of xenobiotics in the body. Compounds that exert toxic effects on the liver are classified as hepatotoxicants [30].

Based on the results of the present investigation, administration of Q-CD-MOF at a dose of 10 mg/kg body weight did not induce hepatotoxic effects in the test animals (mice). Histopathological analysis (Figure 11) revealed no observable differences in hepatic architecture between treated and untreated groups. Specifically, there were no indications of steatosis, necrosis, cholestasis, hepatitis, or hepatocellular carcinoma. These findings clearly indicate that the potassium–cyclodextrin linker forming the CD-MOF as a quercetin delivery system does not elicit hepatotoxicity *in vivo*.

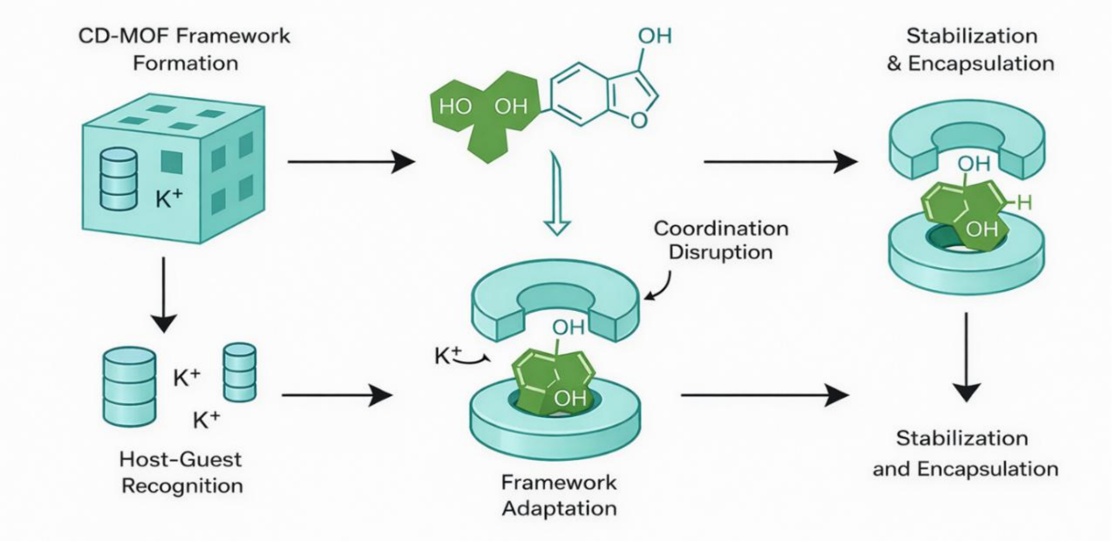

Figure 11. Mechanism of Host-Guest interaction Cyclodextrin-Quarcetin

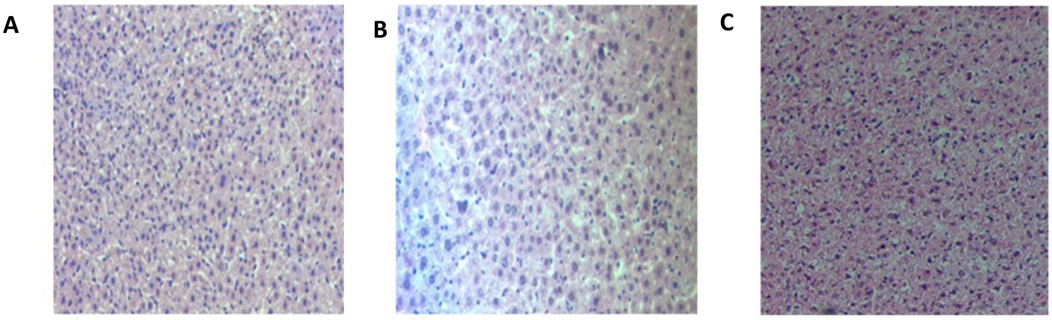

Figure 12. Histological analysis of liver tissues: (A) Q–CD-MOF, (B) quercetin, and (C) normal control, showing well-preserved hepatic structures and confirming the biocompatibility of Q–CD-MOF

Conclusion

This study successfully synthesized and modified β-CD-MOF using cetyltrimethylammonium bromide (CTAB), resulting in a functional carrier specifically optimized for quercetin delivery. Comprehensive characterization (FTIR, XRD, SEM-EDS, and PSA) confirmed the formation of a porous crystalline framework, effective CTAB surface modification, and successful quercetin encapsulation. The release study demonstrated a clear biphasic profile, with an initial burst phase followed by a diffusion-controlled sustained release up to 120 min. Antioxidant evaluation showed that Q-CD-MOF maintained 90.92% inhibition, closely comparable to free quercetin, confirming that encapsulation preserved its biological activity. In vivo histopathological assessment indicated no detectable hepatotoxicity at the tested dose (10 mg/kg BW), suggesting good preliminary biocompatibility; however, further dose–response and long-term studies are necessary before broader biological applications.

Acknowledgements

The authors would like to express their sincere gratitude to the Faculty of Science and Technology, Universitas Jambi, for providing laboratory facilities, and to the Institute for Research and Community Service (LPPM), Universitas Jambi, for its invaluable support.

Funding

This research was funded by the Directorate of Research, Technology, and Community Service (DRTPM), Ministry of Higher Education, Science, and Technology of Indonesia, under decree No. 071/C3/DT.05.00/PL/2025 with contract number 18/UN21.11/PT.01.05/SPK.2025. The authors also acknowledge the support of the Natural Products and Bioactive Compounds Laboratory for additional funding.

Conflict of Interest

Authors declared no conflict of interest in this work.

ORCID

Muhammad Furqon Novryan Saputra
https://orcid.org/0009-0002-3298-8482
Aliyah Nabila
https://orcid.org/0009-0005-0958-0069
Madyawati Latief
https://orcid.org/0000-0001-6023-4640
Ayu Nadila Safitri
https://orcid.org/0000-0003-3820-7931
Indra Lasmana Tarigan
https://orcid.org/0000-0002-7238-7780

References

[1] Rojas, S., Devic, T., Horcajada, P. Metal organic frameworks based on bioactive components. *Journal of Materials Chemistry B*, **2017**, 5(14), 2560-2573.

[2] Khafaga, D.S., El-Morsy, M.T., Faried, H., Diab, A.H., Shehab, S., Saleh, A.M., Ali, G.A. Metal–organic frameworks in drug delivery: engineering versatile platforms for therapeutic applications. *RSC Advances*, **2024**, 14(41), 30201-30229.

[3] Zayeri, A., Zahedi Asl, S., Mehrasa, S., Hooriabad Saboor, F., Safajou-Jahankhanemlou, M. Semiconductor gas sensors based on hollow metal oxides: Focusing on MOF-derived structures. *Progress in Chemical and Biochemical Research*, **2025**, 8(3), 304-329.

[4] Li, W., Zou, T., Wang, Z., Zhang, Y., Zhang, J. Fabrication of ultra-stable boronic acid-functionalized quinoline-linked COF for selective adsorption of quercetin. *Analytica Chimica Acta*, **2025**, 344286.

[5] Chen, Y., Su, J., Dong, W., Xu, D., Cheng, L., Mao, L., Yuan, F. Cyclodextrin-based metal–organic framework nanoparticles as superior carriers for curcumin: Study of encapsulation mechanism, solubility, release kinetics, and antioxidative stability. *Food Chemistry*, **2022**, 383, 132605.

[6] Guo, Z., Xiao, Y., Wu, W., Zhe, M., Yu, P., Shakya, S., Xing, F. Metal–organic framework-based smart stimuli-responsive drug delivery systems for cancer therapy: advances, challenges, and future perspectives. *Journal of Nanobiotechnology*, **2025**, 23(1), 157.

[7] Escobar-Avello, D., Avendaño-Godoy, J., Santos, J., Lozano-Castellón, J., Mardones, C., von Baer, D., Gómez-Gaete, C. Encapsulation of phenolic compounds from a grape cane pilot-plant extract in hydroxypropyl beta-cyclodextrin and maltodextrin by spray drying. *Antioxidants*, **2021**, 10(7), 1130.

[8] Paiva-Santos, A.C., Ferreira, L., Peixoto, D., Silva, F., Soares, M.J., Zeinali, M., Mazzola, P.G. Cyclodextrins as an encapsulation molecular strategy for volatile organic compounds—Pharmaceutical applications. *Colloids and Surfaces B: Biointerfaces*, **2022**, 218, 112758.

[9] Sadeh, P., Zeinali, S., Rastegari, B., Najafipour, I. Functionalization of β-cyclodextrin metal-organic frameworks with gelatin and glutamine for drug delivery of curcumin to cancerous cells. *Heliyon*, **2024**, 10(9).

[10] Martínez-Mendoza, B.I., Juárez-Trujillo, N., Mendoza-Lopez, M.R., Monribot-Villanueva, J.L., Guerrero-Analco, J.A., Jiménez-Fernández, M. Bioactive compounds, antioxidant and antibacterial properties of the pulp, peel and aril of the fruit of Clusia quadrangula (Clusiaceae). *Acta Botánica Mexicana*, **2023**, 130.

[11] Mutha, R.E., Tatiya, A.U., Surana, S.J. Flavonoids as natural phenolic compounds and their role in therapeutics: An overview. *Future Journal of Pharmaceutical Sciences*, **2021**, 7(1), 25.

[12] Pei, S., Dou, Y., Zhang, W., Qi, D., Li, Y., Wang, M., Yao, C. *O*-Sulfation disposition of curcumin and quercetin in SULT1A3 overexpressing HEK293 cells: the role of arylsulfatase B in cellular *O*-sulfation regulated by transporters. *Food & Function*, **2022**, 13(20), 10558-10573.

[13] Saputra, M.F.N., Nabila, A., Maulida, F., Ramadhani, S., Syafiq, M.H., Tarigan, I.L. Synthesis and characterization of insulin-MOF-5 loaded into cellulose nanocrystalline-based dissolving microneedle as anti-diabetic delivery system. *Journal of Medicinal and Chemical Sciences*, **2025**, 8(2), 177-189.

[14] Vijayakumar, B.G., Ramesh, D., Joji, A., Kannan, T. *In silico* pharmacokinetic and molecular docking studies of natural flavonoids and synthetic indole chalcones against essential proteins of SARS-CoV-2. *European Journal of Pharmacology*, **2020**, 886, 173448.

[15] Seke, F., Adiamo, O.Q., Sultanbawa, Y., Sivakumar, D. In vitro antioxidant activity, bioaccessibility, and thermal stability of encapsulated strawberry fruit (*Fragaria× ananassa*) polyphenols. *Foods*, **2023**, 12(21), 4045.

[16] Arvelo, D.M., Comer, J., Schmit, J., Garcia, R. Interfacial water is separated from a hydrophobic silica surface by a gap of 1.2 nm. *ACS Nano*, **2024**, 18(28), 18683-18692.

[17] Gutiérrez, M., Zhang, Y., Tan, J.C. Confinement of luminescent guests in metal–organic frameworks: understanding pathways from synthesis and multimodal characterization to potential applications of LG@MOF systems. *Chemical Reviews*, **2022**, 122(11), 10438-10483.

[18] Mirza, M.A., Mahmood, S., Hilles, A.R., Ali, A., Khan, M.Z., Zaidi, S.A.A., Ge, Y. Quercetin as a therapeutic product: evaluation of its pharmacological action and clinical applications—a review. *Pharmaceuticals*, **2023**, 16(11), 1631.

[19] Sajjadifar, S., Abakhsh, F., Arzehgar, Z. Design and Characterization of Fe_3O_4@*n*Pr-NH_2@$Zn_3(BTC)_2$ Magnetic MOF: A Catalyst for Dihydropyrimidine and 2-Amino-4*H*-Chromene Synthesis. *Chemical Methodologies*, **2024**, 8(8), 550-568.

[20] Tatrari, G., An, R., Shah, F.U. Designed metal-organic framework composites for metal-ion batteries and metal-ion capacitors. *Coordination Chemistry Reviews*, **2024**, 512, 215876.

[21] Rahman, M., Kabir, M., Islam, T., Wang, Y., Meng, Q., Liu, H., Wu, S. Curcumin-loaded ZIF-8 nanomaterials: exploring drug loading efficiency and biomedical performance. *ACS omega*, **2025**, 10(3), 3067-3079.

[22] Li, Q.J., Xing, F., Wu, W.T., Zhe, M., Zhang, W.Q., Qin, L., Fan, M.H. Multifunctional metal–organic frameworks as promising nanomaterials for antimicrobial strategies. *Burns & Trauma*, **2025**, 13, tkaf008.

[23] Rajamohan, R., Raorane, C.J., Kim, S.C., Krishnan, M.M., Lee, Y.R. Supramolecular *β*-cyclodextrin-quercetin based metal–organic frameworks as an efficient antibiofilm and antifungal agent. *Molecules*, **2023**, 28(9), 3667.

[24] Listyaningrum, R.S., Adi, P., Mulyani, R., Tsai, S.Y., Yudhistira, B., Hsieh, C.W. Current status and future directions on cyclodextrin-based metal–organic frameworks for adsorption and controlled release of gaseous/volatiles in active food packaging. *Trends in Food Science & Technology*, **2025**, 105456.

[25] Murugesan, A., Li, H., Shoaib, M. Recent advances in functionalized carbon quantum dots integrated with metal–organic frameworks: emerging platforms for sensing and food safety applications. *Foods*, **2025**, 14(12), 2060.

[26] Wang, Z., Ma, Y., Jiang, Y., Zhou, F., Wu, Y., Jiang, H., Hua, C. Encapsulating quercetin in cyclodextrin metal–organic frameworks improved its solubility and bioavailability. *Journal of the Science of Food and Agriculture*, **2022**, 102(9), 3887-3896.

[27] Saxena, S., Lis, M.J. Native cyclodextrin-based Metal–Organic Frameworks (MOFs): Synthesis, characterization, and potential applications in food industry. *Molecules*, **2025**, 30(2), 293.

[28] Dissanayake, T., Bandara, N. Protein-based encapsulation systems for codelivery of bioactive compounds: Recent studies and potential applications. *Current Opinion in Food Science*, **2024**, 57, 101181.

[29] Zhuang, X., Li, L., Liu, T., Zhang, R., Yang, P., Wang, X., Dai, L. Mechanisms of isoniazid and rifampicin-induced liver injury and the effects of natural medicinal ingredients: A review. *Frontiers in Pharmacology*, **2022**, 13(1037814.

[30] Choi, K., Lee, S., Yoo, S., Han, H.Y., Park, S.-y., Kim, J.Y. Prediction of bioactive compounds hepatotoxicity using in silico and in vitro analysis. *Applied Biological Chemistry*, **2024**, 67(1), 107.

HOW TO CITE THIS ARTICLE

M.F.N. Saputra, A. Nabila, M. Latief, A.N. Safitri, I.L. Tarigan, β-Cyclodextrin-Based Metal–Organic Framework as a Novel Functional Bioactive Carrier: A Study for Quercetin Delivery. *Adv. J. Chem. A*, 2026, 9(6), 997-1013.

DOI: 10.48309/ajca.2026.558546.1966
URL: https://www.ajchem-a.com/article_238540.html